

# **Project Report on**

## **Design and Simulation of DC to DC Converter for PV system**

*submitted by*  
**Nair Sabari Vijayan[FIT18EE029]**  
*under the guidance of*  
**Ms. Rakhee R**

*towards partial fulfillment of the requirements for the award of the degree of*  
**Bachelor of Technology**  
**in**  
**Electrical and Electronics Engineering**



**Department of Electrical and Electronics Engineering**  
**Federal Institute of Science And Technology (FISAT)®**  
**Cochin - 683577**

**Affiliated to**  
**APJ Abdul Kalam Technological University, Kerala**  
**Thiruvananthapuram - 695016**

**2021 - 2022**

**Department of Electrical and Electronics Engineering  
Federal Institute of Science And Technology (FISAT)®**

**Cochin - 683577**

**Affiliated to**

**APJ Abdul Kalam Technological University, Kerala  
Thiruvananthapuram - 695016**



## **CERTIFICATE**

*This is to certify that this report entitled **Design and Simulation of DC to DC Converter for PV System** is a bonafide record of the work carried out as part of the final project, during the B.Tech Program by **Nair Sabari Vijayan** towards the partial fulfillment of the requirements for the award of degree of **Bachelor of Technology**, under our guidance and supervision.*

Project Guide

Head of the Department

Date:

Place: Cochin

Internal Examiner

External examiner

## **Abstract**

*Renewable sources of energy and Distributed Generation are the emerging technology nowadays. Due to the unprecedented decline in the availability of natural resources there is an increasing concern on how to produce electricity to keep up with the world's demand. Hence as an alternative we have opted to switch to non - conventional sources of energy like solar energy, wind energy, etc to produce electricity. The most leading technology being electricity produced from solar energy through solar panels. A major challenge for such PV systems is the low voltage conversion ratio of the dc-dc converter used in the system with a maximum efficiency of 15%. A dc-dc converter with high voltage gain and low voltage stress is important for PV applications since it plays a decisive role on how much output we are able to gain from the PV system. DC-DC boost converters with better performances, including improved voltage gain, efficiency, power density, and reliability, are urgently needed for wide conversion range applications. A detailed discussion for the design and simulation of a single-inductor boost converter (SLBC) with ultrahigh voltage boosting capability which can be employed to make the system more efficient is being discussed in this project.*

## **Acknowledgements**

*It is a great opportunity to express our sincere thanks to all those people who have helped us in the process of study of our project topic through their support, encouragement and guidance. We are deeply indebted to express our profound gratitude to Dr. Manoj George, our Principal and the management for providing all the facilities required amidst the pandemic situation prevailing across the state. It is a great privilege to express our sincere thanks to Dr. Archana R, Head of the Department of Electrical and Electronics Engineering for her constant support and encouragement. We would like to place on record our deep sense of gratitude to Ms. Rakhee R, Assistant Professor(Special Grade), Department of Electrical and Electronics Engineering for her general guidance, help and useful suggestions. We would also like to thank all the Faculty of Department of Electrical and Electronics Engineering for their constant support without which this work would not have been possible.*

# Contents

<b>1</b>	<b>Introduction</b>	<b>1</b>
1.1	Photovoltaic System . . . . .	1
1.2	DC-DC Converters . . . . .	2
1.3	Boost Converters . . . . .	3
1.4	Characteristics of Converters . . . . .	3
1.5	Problem Identification . . . . .	4
1.6	Proposal . . . . .	4
1.7	Objective . . . . .	4
<b>2</b>	<b>Literature Review</b>	<b>5</b>
2.1	Similar Approaches . . . . .	5
2.2	Proposed Design . . . . .	6
2.2.1	Performance Comparisons . . . . .	8
2.2.2	Comparison of various parameters between proposed SLBC and Various converters . . . . .	10
<b>3</b>	<b>Design Parameters For The Circuit Elements</b>	<b>11</b>
3.1	Design Parameters . . . . .	11
3.2	Duty Cycle . . . . .	11
3.3	Load Resistance . . . . .	12
3.4	Inductor . . . . .	13
3.4.1	Inductor Winding . . . . .	13
3.5	Capacitor . . . . .	19

<b>4 Simulation</b>	<b>21</b>
4.1 Output Voltage . . . . .	22
4.2 Inductor Current . . . . .	23
4.3 Output Current . . . . .	24
4.4 Voltage Stress . . . . .	25
<b>5 Hardware</b>	<b>26</b>
5.1 Arduino . . . . .	26
5.2 Switch . . . . .	26
5.3 Gate Drive Circuit . . . . .	27
5.4 Diode . . . . .	28
5.5 Snubber Circuit . . . . .	29
<b>6 Software</b>	<b>30</b>
6.1 MatLab . . . . .	30
6.2 Arduino . . . . .	30
6.3 AutoDesk Eagle . . . . .	31
<b>7 Implementation</b>	<b>32</b>
7.1 Circuit Design . . . . .	32
7.1.1 Boost Converter Design . . . . .	32
7.1.2 Control Circuit . . . . .	33
7.2 Prototype . . . . .	33
<b>8 Observation</b>	<b>36</b>
<b>9 Conclusion</b>	<b>38</b>
<b>10 Possible Improvements and Future Works</b>	<b>39</b>

# List of Figures

2.1	Topological Structure of the SLBC . . . . .	6
2.2	Equivalent circuits of the SLBC. (a) State 1. (b) State 2. . . . .	7
2.3	Typical waveforms of the SLBC in CCM . . . . .	8
2.4	Voltage gain versus duty cycle among converters . . . . .	9
4.1	Simulink circuit diagram. . . . .	21
4.2	Output Voltage Waveform . . . . .	23
4.3	Inductor Current Waveform . . . . .	24
4.4	Output Current Waveform . . . . .	24
4.5	Waveform of voltage stress across the switches. . . . .	25
5.1	IRFP4668Pbf . . . . .	27
5.2	Control Circuit . . . . .	28
5.3	MUR 1560 . . . . .	29
5.4	MBR 20200CT . . . . .	29
7.1	Circuit Diagram of proposed DC-DC Converter . . . . .	32
7.2	Control Circuit . . . . .	33
7.3	Prototype of the proposed Boost Converter . . . . .	34
7.4	Prototype of the proposed Boost Converter . . . . .	34
7.5	Prototype of the proposed Boost Converter . . . . .	35
8.1	Gate pulse . . . . .	37

# List of Tables

2.1	Comparison table of various converters . . . . .	10
3.1	Design parameters for the selected converter . . . . .	11
3.2	Various ferrite cores . . . . .	15
3.3	Wire Size Table . . . . .	18
4.1	Circuit Parameters and their values . . . . .	22
8.1	Circuit Parameters and their values . . . . .	36

# **Chapter 1**

## **Introduction**

### **1.1 Photovoltaic System**

A photovoltaic system, also PV system or solar power system, is an electric power system designed to supply usable solar power by means of photovoltaics. It consists of an arrangement of several components, including solar panels to absorb and convert sunlight into electricity, a solar inverter to convert the output from direct to alternating current, as well as mounting, cabling, and other electrical accessories to set up a working system. It may also use a solar tracking system to improve the system's overall performance and include an integrated battery solution, as prices for storage devices are expected to decline. Strictly speaking, a solar array only encompasses the ensemble of solar panels, the visible part of the PV system, and does not include all the other hardware, often summarized as balance of system (BOS). As PV systems convert light directly into electricity, they are not to be confused with other solar technologies, such as concentrated solar power or solar thermal, used for heating and cooling. PV systems range from small, rooftop-mounted or building-integrated systems with capacities from a few to several tens of kilowatts, to large utility-scale power stations of hundreds of megawatts. Nowadays, most PV systems are grid-connected, while off-grid or stand-alone systems account for a small portion of the market.

Operating silently and without any moving parts or environmental emissions, PV systems have developed from being niche market applications into a mature technology used for mainstream electricity generation. A rooftop system recoups the invested energy for its manufacturing and installation within 0.7 to 2 years and produces about 95 percent of net clean renewable energy over a 30-year service lifetime. Due to the growth of photovoltaic, prices for PV systems have rapidly declined since their introduction. However, they vary by market and the size of the system. In 2014, prices for residential 5-kilowatt systems in the United States were around \$3.29 per watt, while in the highly penetrated German market, prices for rooftop systems of up to 100 kW declined to €1.24 per watt. Nowadays, solar PV modules account for less than half of the system's overall cost, leaving the rest to the remaining BOS-components and to soft costs, which include customer acquisition, permitting, inspection and interconnection, installation labor and financing costs.

## 1.2 DC-DC Converters

A converter is an electrical circuit which accepts a DC input and generates a DC output of a different voltage, usually achieved by high frequency switching action employing inductive and capacitive filter elements.

A power converter is an electrical circuit that changes the electric energy from one form into the desired form optimized for the specific load. A converter may do one or more functions and give an output that differs from the input. It is used to increase or decrease the magnitude of the input voltage, invert polarity, or produce several output voltages of either the same polarity with the input, different polarity, or mixed polarities such as in the computer power supply unit.

The DC to DC converters are used in a wide range of applications including computer power supplies, board level power conversion and regulation, dc motor control circuits and much more.

The converter acts as the link or the transforming stage between the power source and the power supply output. There are several kinds of converters based on the source input voltage and the output voltage and these falls into four categories namely the AC to DC converter known as the rectifier, the AC to AC cycloconverter or frequency changer, the DC to DC voltage or current converter, and the DC to AC inverter.

### 1.3 Boost Converters

A boost converter (step-up converter) is a DC-to-DC power converter that steps up voltage (while stepping down current) from its input (supply) to its output (load). It is a class of switched-mode power supply (SMPS) containing at least two semiconductors (a diode and a transistor) and at least one energy storage element: a capacitor, inductor, or the two in combination. To reduce voltage ripple, filters made of capacitors (sometimes in combination with inductors) are normally added to such a converter's output (load-side filter) and input (supply-side filter). Boost converters are highly nonlinear systems and a wide variety of linear and nonlinear control techniques for achieving good voltage regulation with large load variations have been explored.

### 1.4 Characteristics of Converters

- Ultrahigh voltage boosting capability.
- Lower voltage stress of switches.
- Intrinsic small duty cycle to enhance the system efficiency.
- Single-inductor structure to realize continuous input current and high power density [1].

## 1.5 Problem Identification

High gain DC-DC converters are essential to boost the PV voltage to a level that is required to generate grid voltage. Conventional boost converters cannot be used in such applications because of its inability to provide such high gain. Higher gain means that boost converters will have to operate at higher duty cycle of around 0.9, which makes it inefficient and impossible to get in some extreme cases. Although, input current in interleaved boost converter is divided into two or more phases that reduce the losses of the converter. However, if a voltage gain of more than 5 is required, improved step up topologies are needed.[2]

## 1.6 Proposal

- To design and simulate a DC-DC Converter that has a higher conversion ratio than the conventional boost converters.
- This is achieved while maintaining a lower duty cycle which in turn reduces the losses incurred.

## 1.7 Objective

As an important part of the future intelligent power distribution system, dc microgrid can efficiently and reliably integrate distributed renewable energy generation system, energy storage unit, electric vehicle, and other electric loads. Dc-dc converters, which are the key link to realize energy transfer between the units of dc microgrid, are widely researched and applied recently.

The objective of this project is to design and simulate a boost converter with improved conversion ratio for PV system. To design the filter elements of improved converter and Simulate the circuit in MATLAB. Implementing the prototype of the designed converter and ensuring similar results with that of the simulation.

# Chapter 2

## Literature Review

### 2.1 Similar Approaches

From the various papers referenced most of the converter topologies included the use of switched capacitor or coupled inductors. Coupled inductor converters are one of the typical dc-dc converter topology types. Combining with interleaved strategy, two kinds of transformerless boost converters with lower ripples are presented in “A novel interleaved tristate boost converter with lower ripple and improved dynamic response”[3] and “Interleaved high step-up converter with coupled inductors”[4]. The former converter has better dynamic response and reduced efficiency while the latter converter possesses small duty cycle range and zero current switching. But due to the use of coupled inductors the circuit becomes complex.

- (a) “A three-winding coupled-inductor dc-dc converter topology with high voltage gain and reduced switch stress”[5]
- (b) “Analysis and design of high-efficiency hybrid high step-up dc-dc converter for distributed PV generation systems”[6]
- (c) “Study and analysis of pulsating and non-pulsating input and output current of ultrahigh-voltage gain hybrid dc-dc converters”[7]

The above mentioned converters in (a)–(c) all are single switch structures, but more passive components are needed to construct these topologies.

## 2.2 Proposed Design

Here we are intending to use a single-inductor boost converter (SLBC) shown in (Fig.2.1), which is integrated by the Sheppard–Taylor structure and the switched-capacitor technique is presented and analyzed in detail. The major contributions of the SLBC are: ultrahigh voltage boosting capability, lower voltage stress of switches and intrinsic small duty cycle to enhance the system efficiency, single-inductor structure to realize continuous input current and high power density.

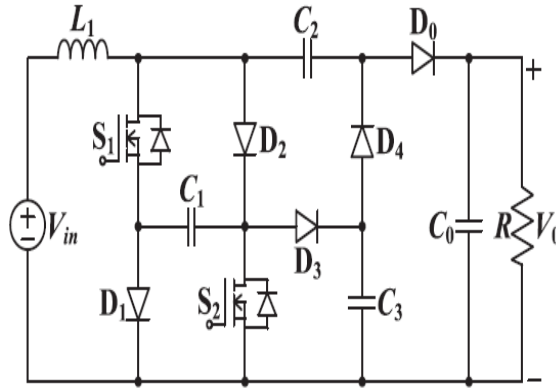


Figure 2.1: Topological Structure of the SLBC

The SLBC is a fifth-order topology, which consists of one input inductor L<sub>1</sub>, three mid-capacitors C<sub>1</sub> to C<sub>3</sub> and one output capacitor C<sub>0</sub>, as shown in (Fig. 2.1). Semiconductors of the SLBC including two synchronously controlled switches S<sub>1</sub> and S<sub>2</sub>, four mid-diodes D<sub>1</sub> to D<sub>4</sub> and one output diode D<sub>0</sub>. The SLBC has two states in CCM basing on the ON-OFF control actions of switches. State 1: As shown in (Fig.2.2 (a)), two synchronously controlled switches S<sub>1</sub> and S<sub>2</sub> together with mid-diode D<sub>4</sub> are ON, the other diodes are OFF in this time interval. There are three circuit loops for the SLBC operating in state 1: L<sub>1</sub>

is magnetized by  $V_{in}$  and  $C_1$  via  $S_1$  and  $S_2$ ; mid-capacitors  $C_1$  and  $C_3$  release energy for  $C_2$  via  $S_1$ ,  $S_2$  and  $D_4$ ;  $C_0$  releases energy for the resistive load  $R$ . State 2: Within this period, the mid-diodes  $D_1$  to  $D_3$  and the output diode  $D_0$  are ON while other switches and diode are OFF, as shown in (Fig.2.2 (b)). Three circuit loops for the SLBC in state 2 are:  $V_{in}$  and  $L_1$  supply energy for  $C_1$  via  $D_1$  and  $D_2$ ;  $V_{in}$  and  $L_1$  supply energy for  $C_3$  via  $D_2$  and  $D_3$ ;  $V_{in}$  together with  $L_1$ ,  $C_2$  supply energy for  $C_0$  and  $R$  via  $D_0$ .

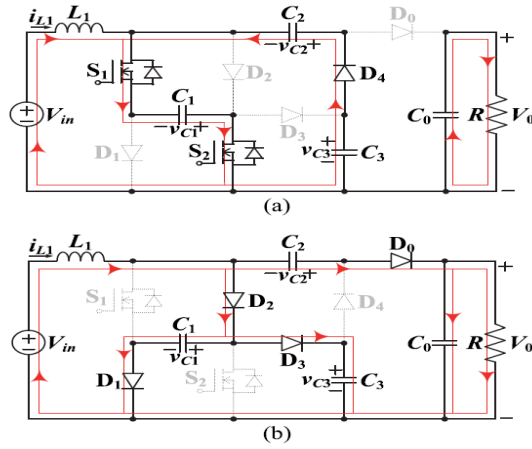


Figure 2.2: Equivalent circuits of the SLBC. (a) State 1. (b) State 2.

Based on the aforementioned operational analyses in state 1, corresponding voltage expressions of the SLBC are listed as follows:

$$\begin{aligned} V_{L1} &= V_{in} + V_{C1} \\ V_{C2} &= V_{C1} + V_{C3}. \end{aligned} \tag{2.1}$$

Similarly, the obtained voltage equations in state 2 are as follows:

$$\begin{aligned} V_{L1} &= V_{in} + V_{C2} - V_0 \\ V_{C1} &= V_{C3} = V_0 - V_{C2}. \end{aligned} \tag{2.2}$$

For  $L_1$ , adopting the volt-second balance and integrating related capacitor voltages in (1) and (2), the derived mid-capacitor voltages and voltage gain of the

SLBC are as follows:

$$V_{C1} = V_{C3} = \frac{1}{1-2D} V_{in} \quad (2.3)$$

$$V_{C2} = \frac{2}{1-2D} V_{in} \quad (2.4)$$

$$M_{CCM} = \frac{V_0}{V_{in}} = \frac{3}{1-2D} V_{in} \quad (2.5)$$

From (3) to (5), it is clear that the operational duty cycle range of the SLBC is  $0 \leq D \leq 0.5$ . Within this range, the SLBC realize low mid-capacitor voltages and ultrahigh voltage gain. When the switches or the diodes are OFF, the voltage stress across them can be obtained as follows:

$$V_{S1} = V_{S2} = V_{D1} = V_{D2} = V_{D3} = \frac{1}{1-2D} V_{in} \quad (2.6)$$

$$V_{D4} = V_{D0} = \frac{2}{1-2D} V_{in} \quad (2.7)$$

(Fig.2.3) shows the typical waveforms of the SLBC in Continuous Conduction Mode (CCM).

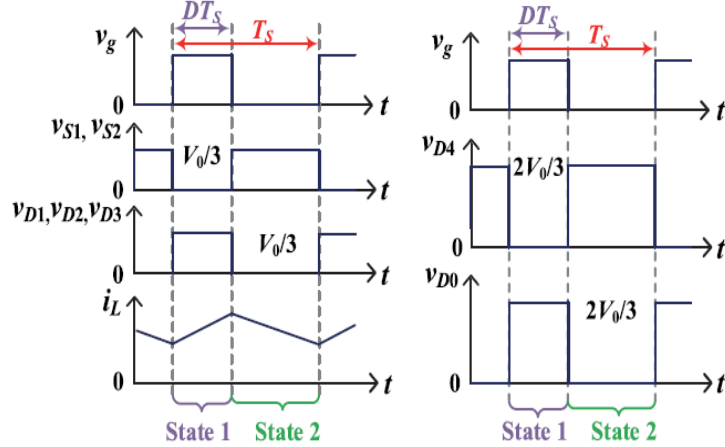


Figure 2.3: Typical waveforms of the SLBC in CCM

### 2.2.1 Performance Comparisons

(Fig.2.4) draws the voltage gain curves verses duty cycle among the various converters taken into consideration. One can see that the voltage gain of the

SLBC is always the highest within the duty cycle range. Moreover, for the SLBC, the obtained voltage gain ranges from 10 to 15 when D varies from 0.35 to 0.4. These duty cycle scopes are far away from the extreme duty cycle and easy to implement on the one hand and small enough to enhance the system efficiency on the other hand.

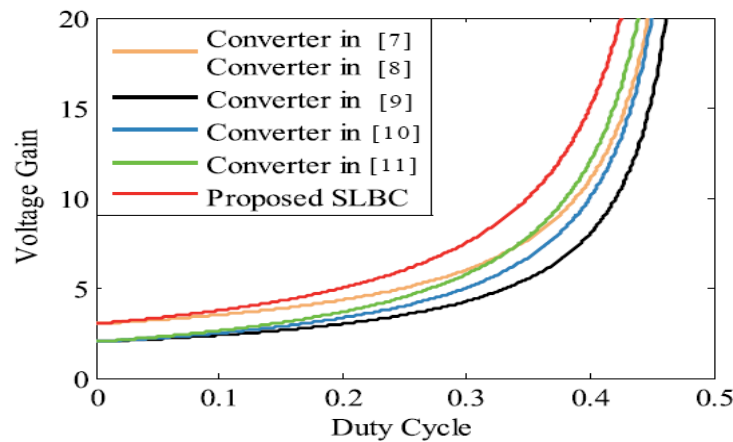


Figure 2.4: Voltage gain versus duty cycle among converters

## 2.2.2 Comparison of various parameters between proposed SLBC and Various converters

	Converter cited as in topologies referred in					
Parameters	[8]	[9]	[10]	[11]	[12]	Proposed SLBC
No. of L/C/S/D	1/3/2/4	2/4/1/3	2/5/1/4	2/6/1/5	3/7/1/5	1/4/2/5
Voltage gain range in CCM	3.5 - 11	2.375 - 8	2.5 - 10	3.5 - 11	2.625 - 12	3.75 - 15
Duty Cycle	0.389	0.421	0.4	0.389	0.38	0.35
Continuous input current	No	No	Yes	No	No	Yes
Common Ground	No	Yes	Yes	Yes	No	Yes

Table 2.1: Comparison table of various converters

# Chapter 3

## Design Parameters For The Circuit Elements

### 3.1 Design Parameters

Parameters	Proposed SLBC
No: of L/C/S/D	1/4/2/5
Voltage Gain in CCM (M)	$\frac{3}{1 - 2D}$
Voltage Gain in CCM ( $D = 0.1 - 0.45$ )	3.75 - 20
Input Voltage ( $V_{in}$ )	12 V
Output Voltage ( $V_0$ )	230 V
Output Power ( $V_0$ )	20 W
Switching Frequency ( $f_s$ )	25 kHz

Table 3.1: Design parameters for the selected converter

### 3.2 Duty Cycle

For the parameters chosen, the duty cycle corresponding to it was found from the following steps :

The input voltage was taken as :

$$V_{in} = 12V \quad (3.1)$$

The output voltage was taken as :

$$V_o = 230V \quad (3.2)$$

The gain of the selected boost converter is given by the equation :

$$\frac{V_o}{V_{in}} = \frac{3}{1 - 2D} \quad (3.3)$$

After substituting the selected values in the equation we get the corresponding duty cycle:

$$\frac{230}{12} = \frac{3}{1 - 2D} \quad (3.4)$$

$$1 - 2D = \frac{3 * 12}{230} = 0.1565 \quad (3.5)$$

$$2D = 0.8434 \quad (3.6)$$

$$D = 0.421 \quad (3.7)$$

### 3.3 Load Resistance

The converter is designed for an output power of :

$$P_0 = 20W \quad (3.8)$$

The load resistance is given by the equation:

$$R_0 = \frac{V_{out}^2}{P_0} \quad (3.9)$$

Substituting the corresponding values in the equation the value of the load resistance is obtained as:

$$R_0 = \frac{230^2}{20} \quad (3.10)$$

$$R_0 = 2645$$

Hence, a standard value of 2700 ohm is taken.

### 3.4 Inductor

From the earlier findings the value of Duty cycle is calculated as follows :

$$D = 0.421 \quad (3.11)$$

The switching time period is found from the switching frequency which is taken as 25kHz in order to increase the efficiency and improve the capacitor values. The percentage ripple for the inductor is taken as 25%.

$$T_s = \frac{1}{F_s} \quad (3.12)$$

$$F_s = 25\text{KHz} \quad (3.13)$$

$$V_o = 230V \quad (3.14)$$

$$I_{L1} = \frac{3}{1 - 2D} I_0 \quad (3.15)$$

$$I_0 = 0.0867A \quad (3.16)$$

Substituting these values in the above mentioned equation gives inductor current as:

$$I_{L1} = 1.17A \quad (3.17)$$

$$\%I_{L1} = 1.17 * \frac{25}{100} \quad (3.18)$$

The inductor value is found to be :

$$L_1 \geq \frac{2D * (1 - D) * V_o * T_s}{3 * \%I_{L1}} \geq 5.102 * 10^{-3} \quad (3.19)$$

Hence the value of inductor is taken as 5.6 mH

#### 3.4.1 Inductor Winding

$$L = 5.6mH \quad (3.20)$$

Energy stored in the inductor;

$$E_L = \frac{L * I_M * I_M}{2} \quad (3.21)$$

$$E_L = 0.0472 \quad (3.22)$$

Area Product of inductor core:

$$A_p = \frac{2 * E_L}{k_w * k_c * J * B_m} \quad (3.23)$$

$k_w = 0.6$  (for single winding inductor)

$k_c$  = peak factor of inductor current

$J$  = current density =  $3*10^6$  A/m<sup>2</sup>

$$A_p = 198900 \text{ mm}^4 \quad (3.24)$$

Cores without air gap	Mean length per turn (mm)	Core cross-section area, $A_c(\text{mm}^2)$	Window Area, $A_w(\text{mm}^2)$	Area product, $A_p(\text{mm}^4)$
POT CORES				
P18/11	35.6	43	27	1161
P26/16	52	94	53	4982
P30/19	60	136	75	10200
P36/22	73	201	101	20301
P42/29	86	264	181	47784
P66/56	150	715	518	370370
EE CORES				
E20/10/5	38	31	47.8	1481
E25/9/6	51.2	40	78	3120
E/25/13/7	52	55	87	4785
E30/15/7	56	59.7	119	7104.5
E36/18/11	70.6	131	141	18471
E42/21/9	77.6	107	256	46592

Cores without air gap	Mean length per turn (mm)	Core cross-section area, $A_c(\text{mm}^2)$	Window Area, $A_w(\text{mm}^2)$	Area product, $A_p(\text{mm}^4)$
EE CORES				
E42/21/15	93	182	256	27392
E42/21/20	99	235	256	60160
E65/32/13	150	266	537	142842
UU CORES				
UU15	44	32	59	1888
UU21	55	55	101	5555
UU23	64	61	136	8296
UU60	183	196	1165	228340
UU100	29.3	645	2914	1879530
TOROIDS				
T10	12.8	6.2	19.6	121.52
T12	19.2	12	44.2	530.4
T16	24.2	20	78.5	1570
T20	25.2	22	95	2090
T27	34.1	42	165.1	6934.2
T32	39.6	61	165.1	10071.1
T45	54.7	93	615.7	57260.1

Table 3.2: Various ferrite cores

From the (table.3.2):

$$A_p = 142842mm^4$$

$$L_m = 146.3mm$$

$$A_c = 266mm^2$$

$$A_w = 537mm^2$$

$$Core = E65/32/13$$

Calculation of permeance;

$$Permeance = \frac{\mu_0 * \mu_r * A_c}{L_m + (\mu_r * l_g)} \quad (3.25)$$

$$= 1.85 * 10^{-6} H/turns \quad (3.26)$$

Number of turns of inductor;

$$N = \sqrt{\frac{L}{Permeance}} \quad (3.27)$$

$$= 55 turns \quad (3.28)$$

Calculating the size of copper wire;

$$Area = \frac{I_{rms}}{J} \quad (3.29)$$

$$= 1.36mm^2 \quad (3.30)$$

But due to difficulty in winding of the wire due to its large thickness, the gauge of the wire was switched to 22 so as to properly wind the inductor. Hence the number of turns was found to be around 30 turns to get an inductance of 5.6mH.

<b>SWG</b>	<b>Diameter with Enamel(mm)</b>	<b>Area of bare conductor(<math>\text{mm}^2</math>)</b>	<b>R/km @20°C ohm</b>	<b>Weight (kg/km)</b>
45	0.086	0.003973	4320	0.0369
44	0.097	0.005189	3323	0.0481
43	0.109	0.006569	2626	0.061
42	0.119	0.008107	2127	0.075
41	0.132	0.00981	1758	0.0908
40	0.142	0.011675	1477	0.1079
39	0.152	0.0137	1258	0.1262
38	0.175	0.0184	945.2	0.1679
37	0.198	0.02343	735.9	0.2202
36	0.218	0.02927	589.1	0.2686
35	0.241	0.03575	482.2	0.3281
34	0.264	0.04289	402	0.3932
33	0.287	0.05067	340.3	0.465
32	.307	0.0591	291.7	0.5408
31	0.33	0.06818	252.9	0.6245
30	0.351	0.07791	221.3	0.7121
29	0.384	0.09372	184	0.8559
28	0.417	0.111	155.3	1.014
27	0.462	0.1363	126.5	1.245
26	0.505	0.1642	105	1.499
25	0.561	0.2027	85.1	1.851
24	0.612	0.2452	70.3	2.233
23	0.665	0.2919	59.1	2.655

SWG	Diameter with Enamel(mm)	Area of bare conductor( $\text{mm}^2$ )	R/km @20°C ohm	Weight (kg/km)
22	0.77	0.3973	43.4	3.607
21	0.874	0.5189	33.2	4.702
20	0.978	0.6567	26.3	5.939
19	1.082	0.8107	21.3	7.324
18	1.293	1.167	14.8	10.537
17	1.501	1.589	10.8	14.313
16	1.709	2.075	8.3	18.678
15	1.92	2.627	6.6	23.64
14	2.129	3.243	5.3	29.15
13	2.441	4.289	4	38.56
12	2.756	5.48	3.1	49.22
11	3.068	6.818	2.5	61
10	3.383	8.302	2.1	74
9	3.8	10.51	1.6	94
8	4.219	12.97	1.3	

Table 3.3: Wire Size Table

From (table 3.3)

$$\text{Area} = 0.3973 \text{ mm}^2 \quad (3.31)$$

Corresponding to the area obtained from (table 3.3)

$$\text{Diameter} = 0.77 \text{ mm}$$

$$\text{SWG} = 22$$

### 3.5 Capacitor

From equation (3.10) it has been found that load resistance:

$$R = 2700 \text{ ohm} \quad (3.32)$$

$$V_{C1} = V_{C3} = 77.27V \quad (3.33)$$

$$V_{C2} = 154.54 \quad (3.34)$$

Percentage Ripple for capacitor C1, C2, and C3 is taken as 10%. Hence :

$$\%V_{C1} = \%V_{C3} = 77.27 * \frac{10}{100} \quad (3.35)$$

$$\%V_{C2} = 154.54 * \frac{10}{100} \quad (3.36)$$

Therefore the value of capacitor C1 is obtained from:

$$C_1 \geq \frac{(1 + D) * V_o * T_s}{(1 - 2D) * R * \%ripple * V_{c1}} \quad (3.37)$$

$$\geq 3.96 * 10^{-6} F \quad (3.38)$$

A standard value of 4.7  $\mu\text{F}$  is considered.

The value of capacitor C2 is obtained from:

$$V_{C2} = 154.54 \quad (3.39)$$

$$C_2 \geq \frac{V_o * T_s}{R * \%ripple * V_{C2}} \quad (3.40)$$

$$\geq 2.2 * 10^{-7} F \quad (3.41)$$

A standard value of 0.22  $\mu\text{F}$  is considered.

The value of capacitor C3 is obtained from:

$$V_{C3} = 77.27V \quad (3.42)$$

$$C_3 \geq \frac{V_o * T_s}{R * \% Ripple * v_{C3}} \quad (3.43)$$

$$\geq 4.4 * 10^{-7} F \quad (3.44)$$

A standard value of 0.47  $\mu\text{F}$  is considered.

Percentage Ripple for capacitor C0 is taken as 1%. The value of capacitor C0 is obtained from:

$$V_{C0} = 230V \quad (3.45)$$

$$\% V_{C0} = 230 * \frac{1}{100} \quad (3.46)$$

$$C_0 \geq \frac{D * V_0 * T_s}{R * \% Ripple * V_{C0}} \quad (3.47)$$

$$\geq 6.23 * 10^{-7} F \quad (3.48)$$

A standard value of 0.68  $\mu\text{F}$  is considered.

# Chapter 4

## Simulation

The simulation was executed in Simulink in MATLAB by using the various library functions provided in it. The circuit so formed is shown in (fig. 4.1)

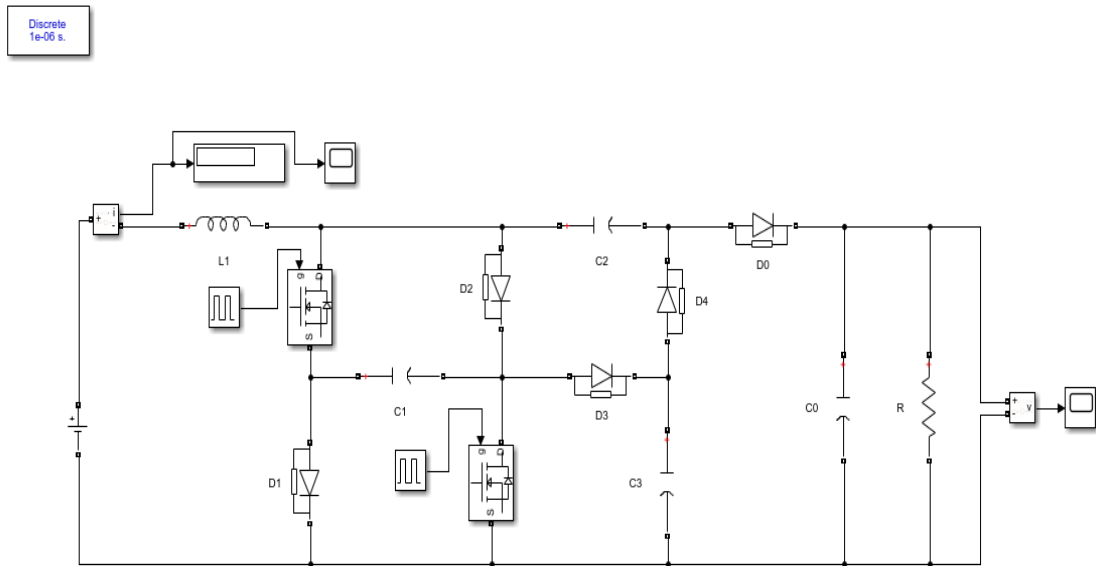


Figure 4.1: Simulink circuit diagram.

The simulation was run under the parameters shown in (table. 4.1):

Circuit Parameters	Parameter Values
Input Voltage	12 V
Inductor	5.6 mH
Pulse Generator frequency	25kHz
Pulse generator Duty Cycle	0.42
Capacitor, C1	4.7 $\mu$ F
Capacitor, C2	0.22 $\mu$ F
Capacitor, C3	0.47 $\mu$ F
Capacitor, C0	0.68 $\mu$ F
Diode - D1, D2, D3	R <sub>on</sub> = 0.001 ohm, V <sub>f</sub> = 0.86 V
Diode - D4, D0	R <sub>on</sub> = 0.001 ohm, V <sub>f</sub> = 1.50 V
Switch - S1, S2	R <sub>on</sub> = 8*10 <sup>-3</sup> ohm, R <sub>d</sub> = 0.01 ohm

Table 4.1: Circuit Parameters and their values

The results of the simulation is shown as graphs in the following sections.

## 4.1 Output Voltage

The simulation is run for a time of 1 second under the parameters mentioned in (table. 4.1) and the following graph is obtained for the output voltage. An output voltage of around 227.6 V is obtained from the circuit which can be seen in (fig. 4.2).

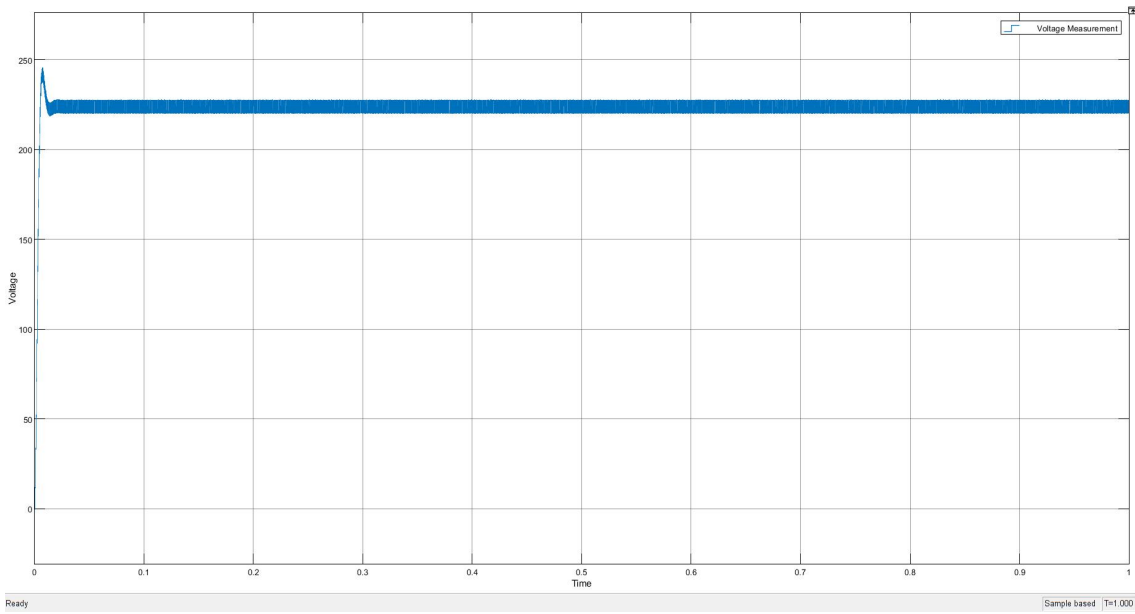


Figure 4.2: Output Voltage Waveform

## 4.2 Inductor Current

The inductor is connected in series with the source and the switch. The inductor current is obtained as around 4.1 A from the display of the simulation. The inductor current waveform is show in the (fig. 4.3)

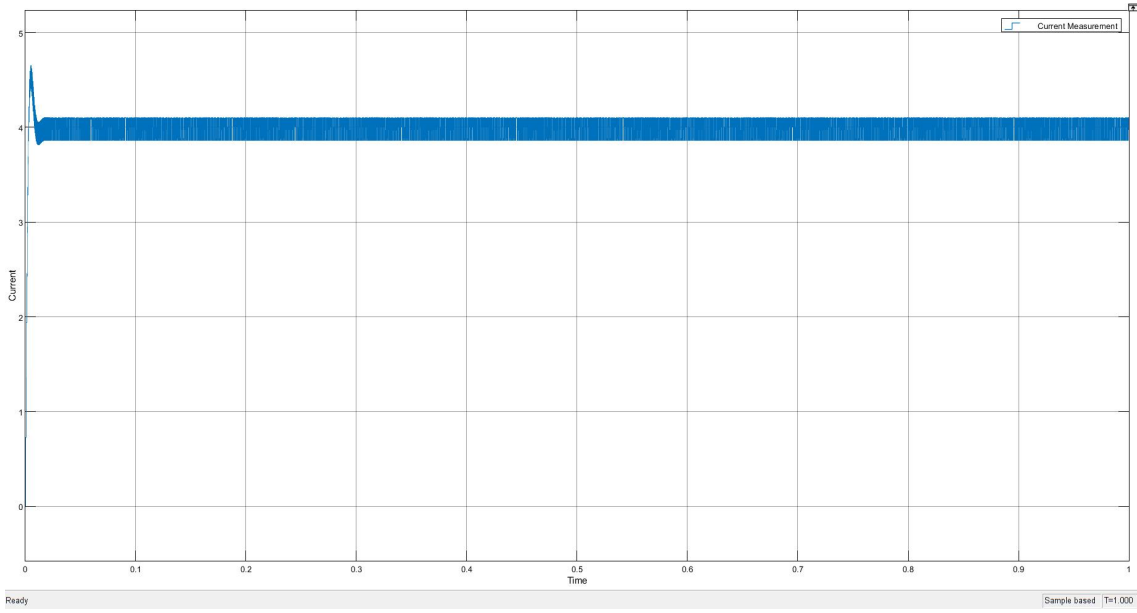


Figure 4.3: Inductor Current Waveform

### 4.3 Output Current

The output current obtained from the output section of the simulation is observed as 0.086 A. The output current waveform is shown in (fig. 4.4).

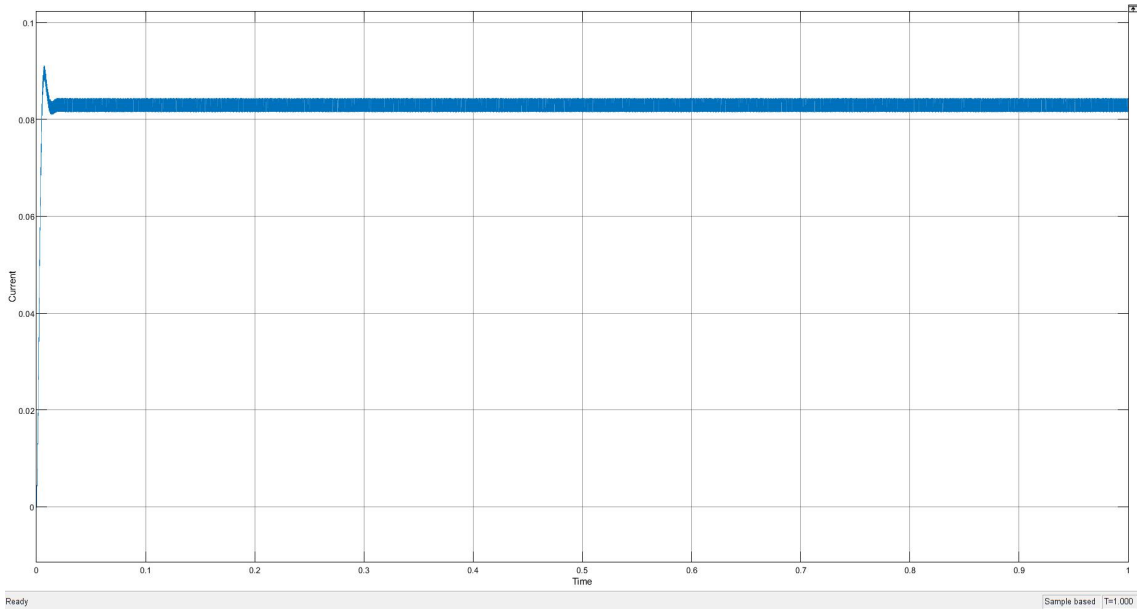


Figure 4.4: Output Current Waveform

## 4.4 Voltage Stress

The voltage stress across the switches is measured when the switches are turned OFF and is observed as around 82.96 V from the display connected across the switches. Since the two switches used are the same, the same voltage is found across the switches when they are turned OFF. The voltage waveform is shown in (fig. 4.5)

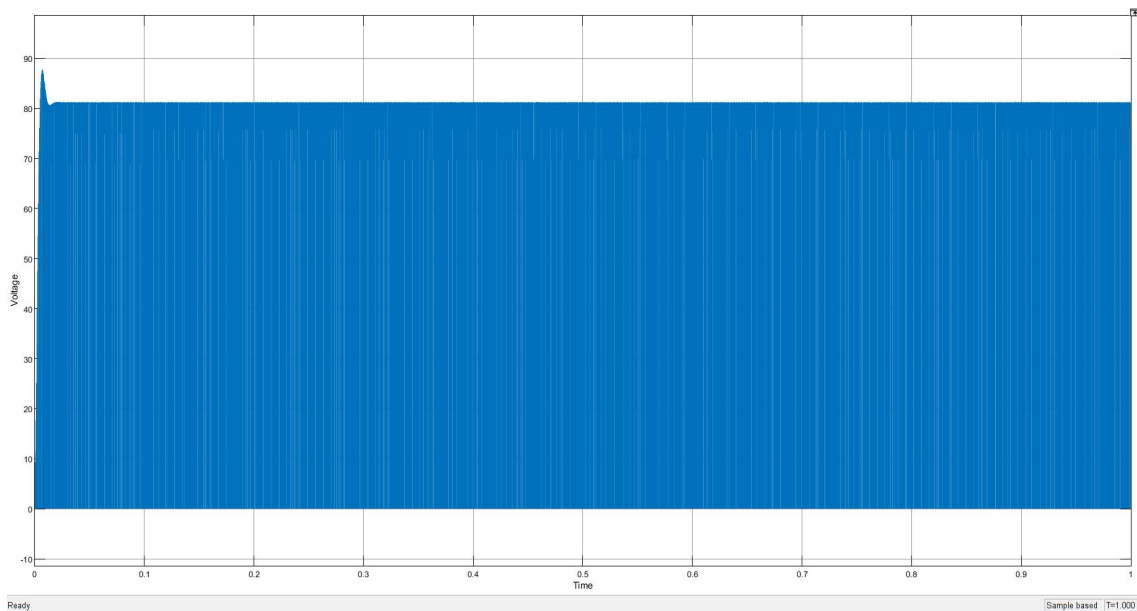


Figure 4.5: Waveform of voltage stress across the switches.

# **Chapter 5**

## **Hardware**

### **5.1 Arduino**

Arduino is an open-source hardware and software company, project and user community that designs and manufactures single-board micro controllers and micro controller kits for building digital devices and interactive objects that can sense and control both physically and digitally.

In this project, Arduino is used to generate the switching frequency to turn on the switches S1 and S2 simultaneously. Frequency generated with the Arduino is 25KHz.

### **5.2 Switch**

Metal Oxide Silicon Field Effect Transistors commonly known as MOSFETs are electronic devices used to switch or amplify voltages in circuits. It is a current controlled device and is constructed by three terminals. The terminals of MOSFET are Source, Gate, Drain and Body. MOSFET was chosen as a better option over other switches due to its low switching losses without disregarding the conduction losses. In this project the switch used is IRFP4668pbF with a Drain - Source Breakdown Voltage of 200V and continuous drain current of 130A, it

has improved Gate, avalanche and dynamic dV/dt along with good ruggedness. It requires a Gate - Source Voltage of 30V to be turned ON and hence requires the help of a Gate drive circuit which provides 30V.



Figure 5.1: IRFP4668Pbf

### 5.3 Gate Drive Circuit

A gate driver is a power amplifier that accepts a low-power input from a controller IC and produces a high-current drive input for the gate of a high-power transistor such as an IGBT or power MOSFET.

A MOSFET usually needs a gate driver to do the on/off operation at the desired frequency. For high frequencies, MOSFETs require a gate drive circuit to translate the on/off signals from an analog or digital controller into the power signals necessary to control the MOSFET. In this project, TLP250H by Toshiba Technologies is used as the gate driver. It can provide a voltage between 20V - 35V. The circuit diagram of the gate drive circuit designed is shown in (fig. 8.1).

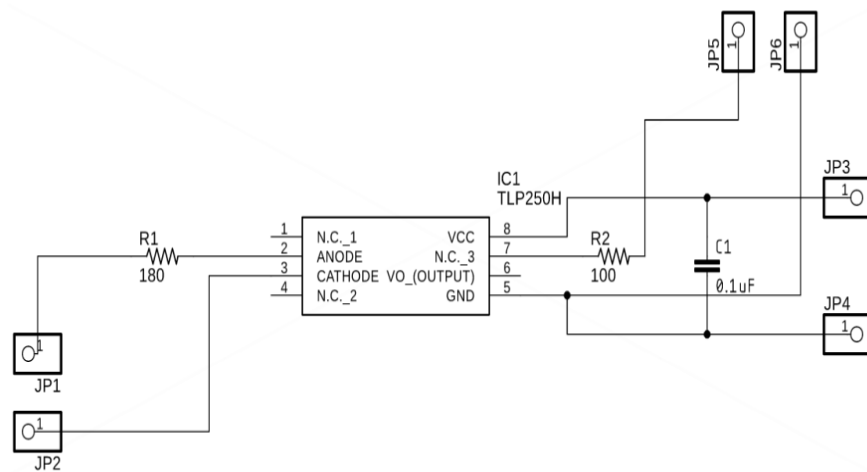


Figure 5.2: Control Circuit

## 5.4 Diode

A diode is a two-terminal electronic component that conducts current primarily in one direction (asymmetric conductance); it has low (ideally zero) resistance in one direction, and high (ideally infinite) resistance in the other. Diodes can be used as rectifiers, signal limiters, voltage regulators, switches, signal modulators, signal mixers, signal demodulators, and oscillators. The fundamental property

of a diode is its tendency to conduct electric current in only one direction. In this project, MBR20200CT and MUR1560 have been used. MBR20200 is a Schottky barrier rectifier with high surge capacity that has a Maximum Peak Reverse Voltage,  $V_{RRM}$  of 200V and a Forward Current,  $I_F$  of 20A shown in (fig. 5.4). MUR1560 is a power rectifier with high voltage capability that has a Maximum Peak Reverse Voltage,  $V_{RRM}$  of 600V and a Forward Current,  $I_F$  of 15A shown in (fig. 5.3).



Figure 5.3: MUR 1560



Figure 5.4: MBR 20200CT

## 5.5 Snubber Circuit

A snubber is a circuit that is used in semiconductor devices for protection and performance enhancements. Here the snubber is a parallel combination of resistor and capacitor connected across each of the MOSFETs. The resistor used in the snubber has a value of  $2k\Omega$  and the capacitor has a value of  $0.47 \mu F$ .

# **Chapter 6**

## **Software**

### **6.1 MatLab**

MATLAB (an abbreviation of "MATrix LABoratory") is a proprietary multi-paradigm programming language and numeric computing environment developed by MathWorks. MATLAB allows matrix manipulations, plotting of functions and data, implementation of algorithms, creation of user interfaces, and interfacing with programs written in other languages. After the design of various elements, it was first simulated in the Matlab, and these results were considered for verification.

### **6.2 Arduino**

Arduino is an open-source hardware and software company, project and user community that designs and manufactures single-board micro controllers and micro controller kits for building digital devices and interactive objects that can sense and control both physically and digitally. Here, the Arduino IDE is used to as an interface to program the Arduino Uno to generate a switching frequency of 25kHz to turn the switches ON and OFF simultaneously.

The program is as shown below:

```
void setup()
{
    DDRD = B11111111; // set PORTD (digital 7 0) to outputs
}
void loop()
{
    PORTD = B11110000; // digital 4 7 HIGH, digital 3 0 LOW
    delayMicroseconds(17);
    PORTD = B00001111; // digital 4 7 LOW, digital 3 0 HIGH
    delayMicroseconds(24);
}
```

### 6.3 AutoDesk Eagle

EAGLE is a scriptable electronic design automation application with schematic capture, printed circuit board layout, auto-router and computer-aided manufacturing features. The circuit design for PCB etching and component footprint was performed with the help of EAGLE for both the converter topology and the two gate drive circuits.

# Chapter 7

## Implementation

### 7.1 Circuit Design

#### 7.1.1 Boost Converter Design

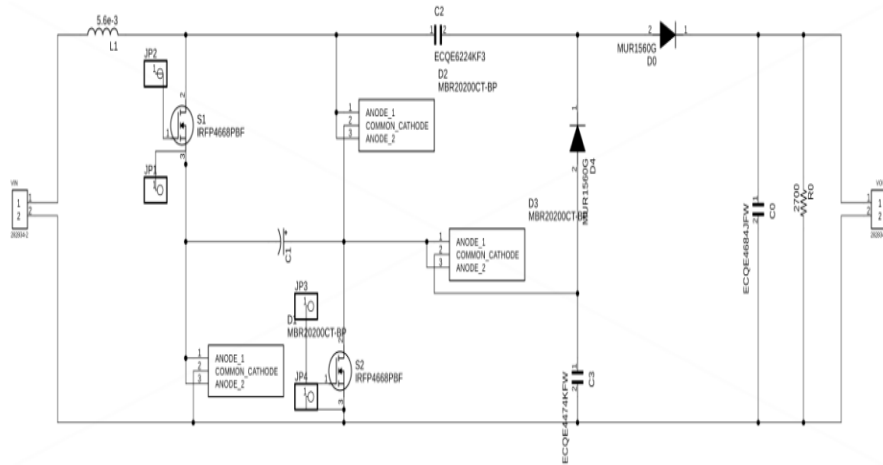


Figure 7.1: Circuit Diagram of proposed DC-DC Converter

### 7.1.2 Control Circuit

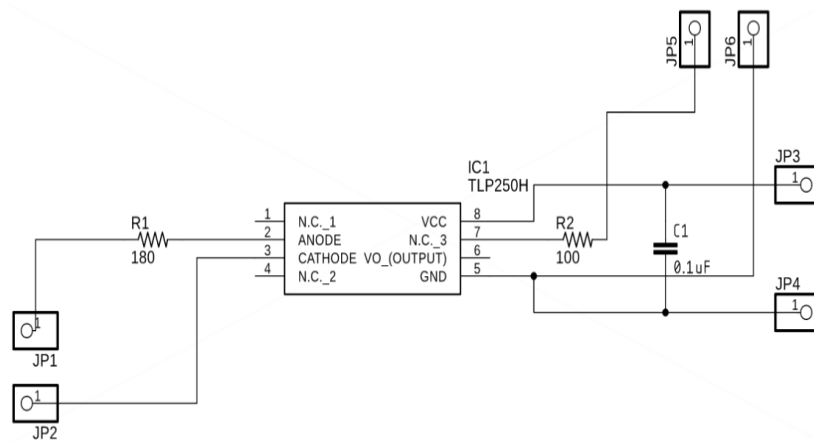


Figure 7.2: Control Circuit

### 7.2 Prototype

The prototype shown in (fig. 7.3) shows the complete circuit including the boost converter and the control circuit.

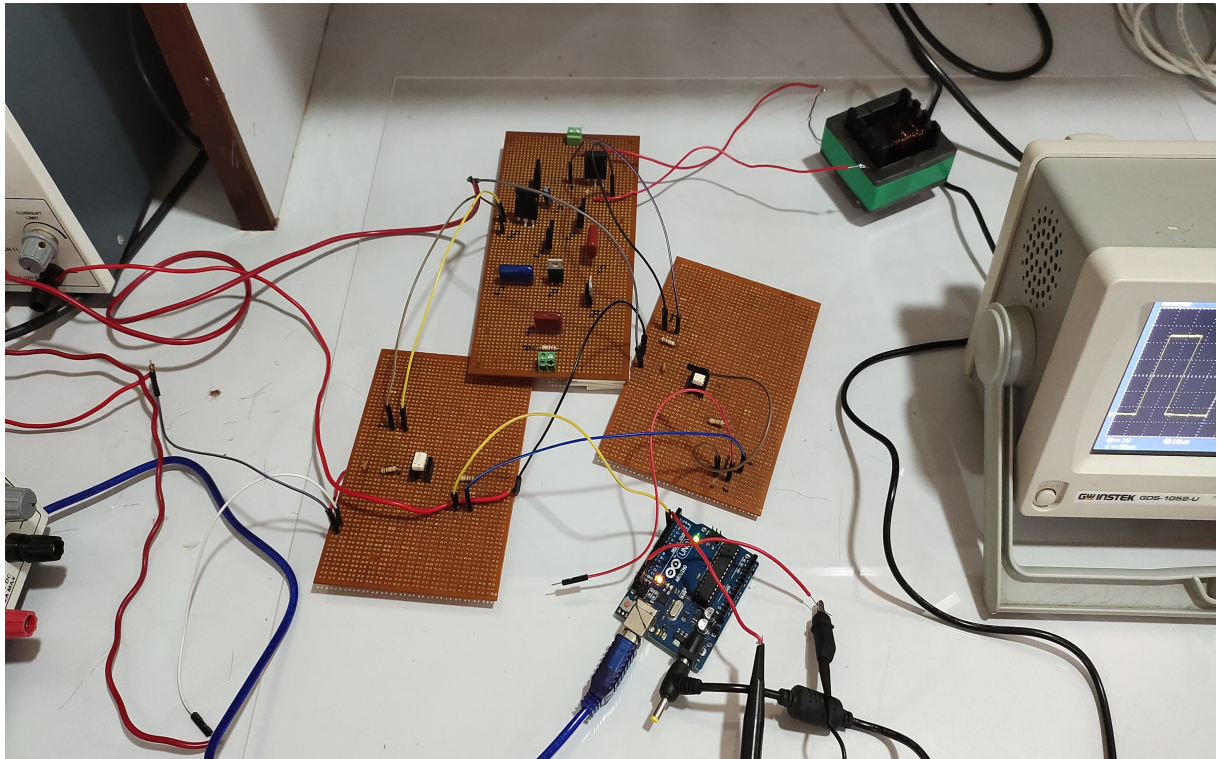


Figure 7.3: Prototype of the proposed Boost Converter

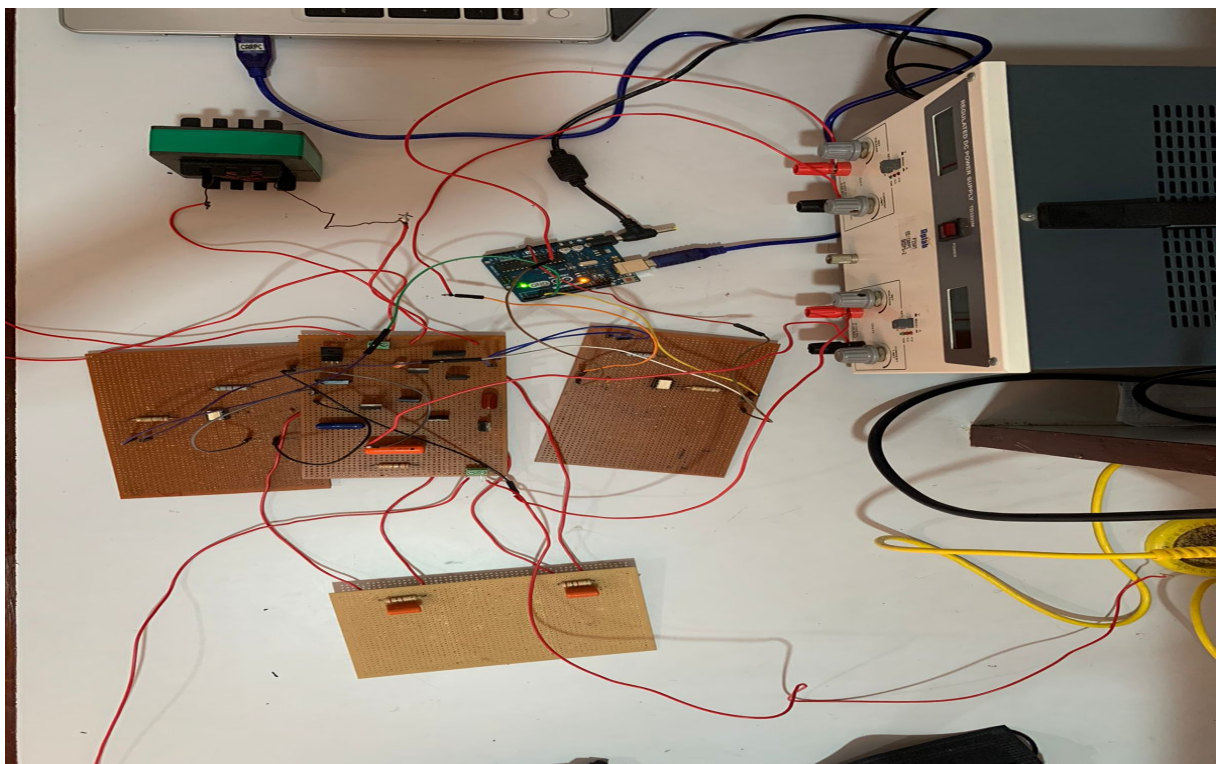


Figure 7.4: Prototype of the proposed Boost Converter

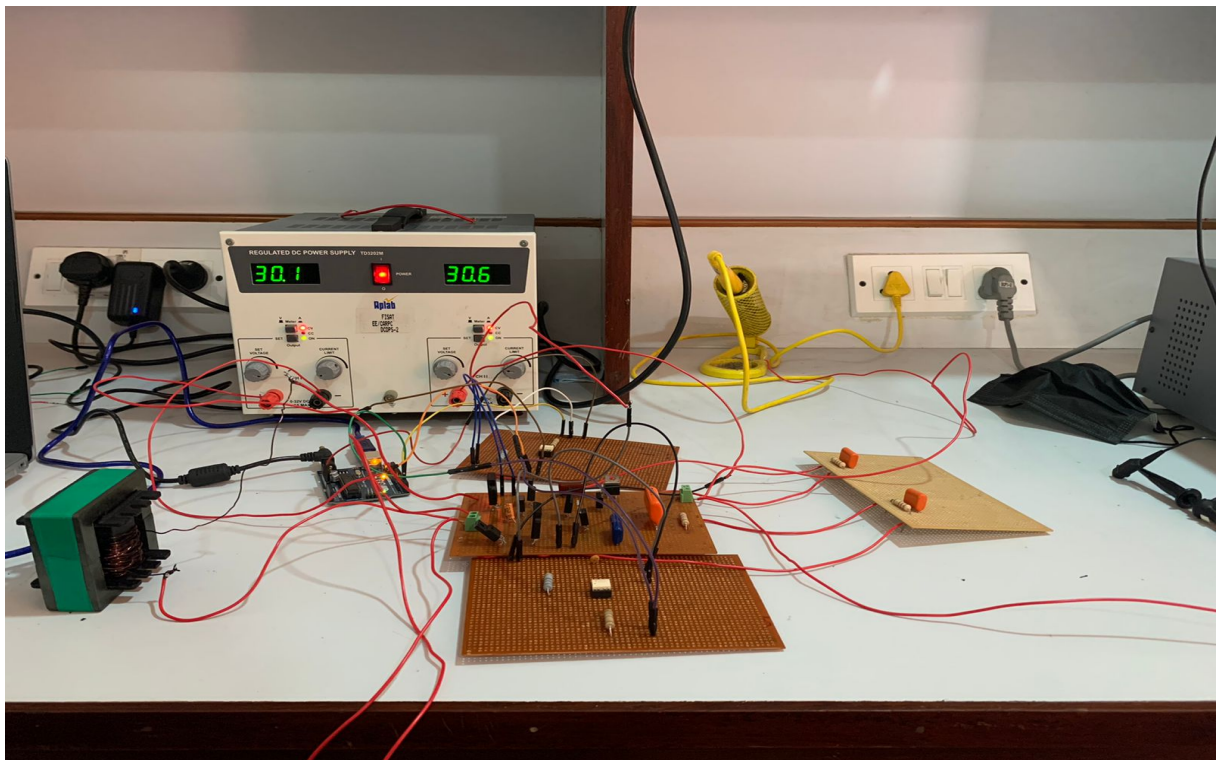


Figure 7.5: Prototype of the proposed Boost Converter

# Chapter 8

## Observation

The proposed circuit diagram was implemented in MATLAB Simulink with the following conditions and parameters shown in (table.8.1)

Circuit Parameters	Parameter Values
Input Voltage	12 V
Inductor	5.6 mH
Pulse Generator frequency	25kHz
Pulse generator Duty Cycle	0.42
Capacitor, C1	4.7 $\mu$ F
Capacitor, C2	0.22 $\mu$ F
Capacitor, C3	0.47 $\mu$ F
Capacitor, C0	0.68 $\mu$ F
Diode - D1, D2, D3	R <sub>on</sub> = 0.001 ohm, V <sub>f</sub> = 0.86 V
Diode - D4, D0	R <sub>on</sub> = 0.001 ohm, V <sub>f</sub> = 1.50 V
Switch - S1, S2	R <sub>on</sub> = 8*10^-3 ohm, R <sub>d</sub> = 0.01 ohm

Table 8.1: Circuit Parameters and their values

After running the simulation for a time period of 1 seconds an output of 227.6 V was observed with stress voltages across the switches being observed as around 87 V. The hardware implementation of the simulation was completed upto the

gate drive pulse generation. The pulse generated was observed to have a value of 30 V and a frequency of 25kHz in the digital oscilloscope as shown in (fig.8.1).



Figure 8.1: Gate pulse

# **Chapter 9**

## **Conclusion**

The design and simulation of the proposed DC-DC converter has been done. The experimental implementation was completed up until the gate drive generation. The simulation results were found to be satisfactory to that of the designed values of the converter. According to the simulation, this DC-DC converter has the following features:

1. Ultrahigh voltage boosting capability without using transformer or coupled-inductor
2. Lower switching losses
3. Simple topological structure
4. Continuous input current

These converters can also be used in applications that desire high voltage gain, high efficiency, high power density, and high reliability.

# **Chapter 10**

## **Possible Improvements and Future Works**

1. The proposed converter has a very low current output, thus to increase the output amperes many panels can be connected in parallel to make up for it to be used to supply an equipment that requires more current.
2. Other trending technologies like solar tracking and MPPT control can be applied to get maximum Power point tracking so as to ensure the panel produces maximum voltage and current at each maximum power point for the corresponding irradiance.

# Bibliography

- [1] Shan Miao, Wei Liu, and Jinfeng Gao. Single-inductor boost converter with ultrahigh step-up gain, lower switches voltage stress, continuous input current, and common grounded structure. *IEEE Transactions on Power Electronics*, 36(7):7841–7852, 2020.
- [2] Bilal Ahmad, Jorma Kyyra, and Wilmar Martinez. Efficiency optimisation of an interleaved high step-up converter. *The Journal of Engineering*, 2019(17):4167–4172, 2019.
- [3] Niraj Rana, Mukesh Kumar, Arnab Ghosh, and Subrata Banerjee. A novel interleaved tri-state boost converter with lower ripple and improved dynamic response. *IEEE Transactions on Industrial Electronics*, 65(7):5456–5465, 2017.
- [4] Yifei Zheng, Wenhao Xie, and Keyue Ma Smedley. Interleaved high step-up converter with coupled inductors. *IEEE Transactions on Power Electronics*, 34(7):6478–6488, 2018.
- [5] Xuefeng Hu, Jianzhang Wang, Linpeng Li, and Yongchao Li. A three-winding coupled-inductor dc–dc converter topology with high voltage gain and reduced switch stress. *IEEE Transactions on Power Electronics*, 33(2):1453–1462, 2017.
- [6] António Manuel Santos Spencer Andrade, Luciano Schuch, and Mário Lúcio da Silva Martins. Analysis and design of high-efficiency hybrid high step-up

- dc–dc converter for distributed pv generation systems. *IEEE Transactions on Industrial Electronics*, 66(5):3860–3868, 2018.
- [7] António Manuel Santos Spencer Andrade and Mário Lúcio da Silva Martins. Study and analysis of pulsating and nonpulsating input and output current of ultrahigh-voltage gain hybrid dc–dc converters. *IEEE Transactions on Industrial Electronics*, 67(5):3776–3787, 2019.
- [8] Minh-Khai Nguyen, Truong-Duy Duong, and Young-Cheol Lim. Switched-capacitor-based dual-switch high-boost dc–dc converter. *IEEE Transactions on Power Electronics*, 33(5):4181–4189, 2017.
- [9] Sajad Rostami, Vahid Abbasi, and Frede Blaabjerg. Implementation of a common grounded z-source dc–dc converter with improved operation factors. *IET Power Electronics*, 12(9):2245–2255, 2019.
- [10] Yun Zhang, Chuanzhi Fu, Mark Sumner, and Ping Wang. A wide input-voltage range quasi-z-source boost dc–dc converter with high-voltage gain for fuel cell vehicles. *IEEE Transactions on Industrial Electronics*, 65(6):5201–5212, 2017.
- [11] Punit Kumar and Mumadi Veerachary. Z-network plus switched-capacitor boost dc–dc converters. *IEEE Journal of Emerging and Selected Topics in Power Electronics*, 2019.
- [12] Mohammad Mehdi Haji-Esmaeili, Ebrahim Babaei, and Mehran Sabahi. High step-up quasi-z source dc–dc converter. *IEEE Transactions on Power Electronics*, 33(12):10563–10571, 2018.